Quantitative Metabolome Profiling of Colon and Stomach Cancer Microenvironment by Capillary Electrophoresis Time-of-Flight Mass Spectrometry

Akiyoshi Hirayama,[1] Kenjiro Kami,[1] Masahiro Sugimoto,[1] Maki Sugawara,[1] Naoko Toki,[1] Hiroko Onozuka,[2] Taira Kinoshita,[2] Norio Saito,[2] Atsushi Ochiai,[2] Masaru Tomita,[1] Hiroyasu Esumi,[2] and Tomoyoshi Soga[1]

[1]Institute for Advanced Biosciences, Keio University, Tsuruoka, Yamagata, Japan and [2]National Cancer Center Hospital East, Kashiwa, Chiba, Japan

Abstract

Most cancer cells predominantly produce energy by glycolysis rather than oxidative phosphorylation via the tricarboxylic acid (TCA) cycle, even in the presence of an adequate oxygen supply (Warburg effect). However, little has been reported regarding the direct measurements of global metabolites in clinical tumor tissues. Here, we applied capillary electrophoresis time-of-flight mass spectrometry, which enables comprehensive and quantitative analysis of charged metabolites, to simultaneously measure their levels in tumor and grossly normal tissues obtained from 16 colon and 12 stomach cancer patients. Quantification of 94 metabolites in colon and 95 metabolites in stomach involved in glycolysis, the pentose phosphate pathway, the TCA and urea cycles, and amino acid and nucleotide metabolisms resulted in the identification of several cancer-specific metabolic traits. Extremely low glucose and high lactate and glycolytic intermediate concentrations were found in both colon and stomach tumor tissues, which indicated enhanced glycolysis and thus confirmed the Warburg effect. Significant accumulation of all amino acids except glutamine in the tumors implied autophagic degradation of proteins and active glutamine breakdown for energy production, i.e., glutaminolysis. In addition, significant organ-specific differences were found in the levels of TCA cycle intermediates, which reflected the dependency of each tissue on aerobic respiration according to oxygen availability. The results uncovered unexpectedly poor nutritional conditions in the actual tumor microenvironment and showed that capillary electrophoresis coupled to mass spectrometry–based metabolomics, which is capable of quantifying the levels of energy metabolites in tissues, could be a powerful tool for the development of novel anticancer agents that target cancer-specific metabolism. [Cancer Res 2009;69(11):4918–25]

Introduction

Most cancer cells are exposed to chronic hypoxia from the early stage of carcinogenesis. Indeed, the measurement of oxygen tension in tumors confirms severe hypoxia in many types of cancer (1). However, cancer cells' predominant use of glycolysis rather than oxidative phosphorylation for energy production, irrespective of oxygen availability (Warburg effect; ref. 2), is widely acknowledged. This indicates that tumor hypoxia is caused not by the excessive oxygen consumption of cancer cells, but rather the inadequate blood supply that results from structurally and functionally defective angiogenesis. In addition, intrinsic characteristics of cancer cells and their constitutive expression of hypoxia-inducible transcription factors activate the genes that encode glycolytic enzymes and glucose transporters (3, 4) and, therefore, jointly hyperactivate glycolysis, to replenish ATP for their continuous growth and proliferation. Nevertheless, the cancer cells' intense use of energy-inefficient glycolysis in the hypovascular microenvironment may deplete glucose from the surrounding tissues. In this manner, the nutritional conditions of the tumor microenvironment may be extremely unfavorable from the perspective of energy metabolism, and significantly different from those that we generally expect from the observation of overgrowing cancer cells.

Although little is known concerning the actual concentrations of glucose and resultant metabolic intermediates in human cancer tissues, the recent development of metabolomics technologies, which are typically based on gas chromatography mass spectrometry (GC-MS; ref. 5), liquid chromatography mass spectrometry (LC-MS; ref. 6), and nuclear magnetic resonance (NMR; ref. 7) is suitable for the large-scale measurement of metabolite levels in tumor and normal tissues. This provides not only direct information on energy metabolism but also the potential reciprocal relationship between metabolic networks and the underlying mechanisms of carcinogenesis.

Recently, metabolome analysis has been applied to the characterization of cancer-cell–specific metabolism. Yang and colleagues (8) applied a computational flux analysis to compare breast cancer and normal human mammary epithelial cell lines by using two-dimensional NMR and GC-MS. Their finding of significant increases in the glycine and proline biosynthesis in cancer cells is interesting, yet may be limited for *in vitro* environment due to its high dependency on culture conditions. Chan and colleagues (9) compared the metabolic profile of biopsied colorectal tumors and their matched normal mucosae obtained from 31 colorectal cancer patients using high-resolution magic angle spinning–NMR and GC-MS and obtained 31 marker metabolites that distinguish normal from malignant samples and further colon from rectal cancers. Moreover, applying GC-MS–based metabolomics, Denkert and colleagues (10) compared the metabolic profiles between invasive ovarian carcinomas and the borderline tumors and between colorectal tumor and pairwise normal tissues (11) and showed that differentially expressed metabolic phenotypes could be exploited

Note: Supplementary data for this article are available at Cancer Research Online (http://cancerres.aacrjournals.org/).

Requests for reprints: Tomoyoshi Soga, Institute for Advanced Biosciences, Keio University, Tsuruoka, Yamagata 997-0052, Japan. Phone: 81-235-29-0528; Fax: 81-235-29-0574; E-mail: soga@sfc.keio.ac.jp.

doi:10.1158/0008-5472.CAN-08-4806

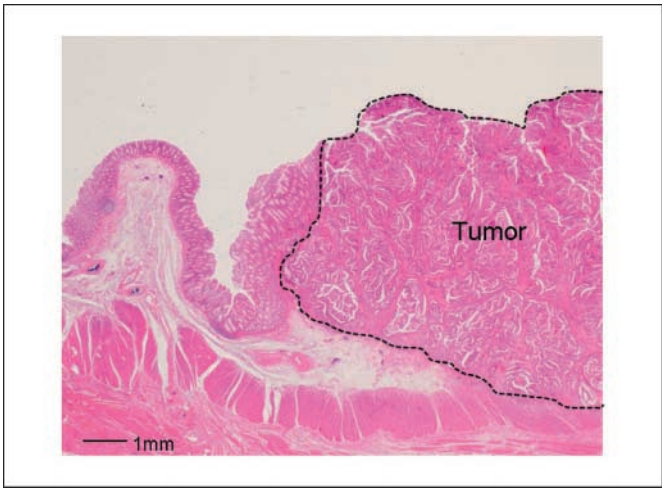

Figure 1. Representative microscopic image of an organ excised from a patient with well-differentiated colorectal adenocarcinoma. Samples were collected from the tumor region (*surrounded by a dotted line*) and nontumor region (considered normal).

to distinguish tumors from the others with high accuracies. However, little has been reported on the quantitation of metabolic intermediates involved in global-scale energy metabolism, including glycolysis, pentose phosphate pathway, and tricarboxylic acid (TCA) cycle, in human cancer and normal tissues. This is mainly due to the lack of effective methodology that allows comprehensive analysis of these metabolites. Most compounds involved in energy metabolism display common properties characterized by high polarity, nonvolatility, and poor detectability, which thus complicates the analysis. We recently developed a state-of-the-art metabolome analysis tool based on capillary electrophoresis coupled to mass spectrometry (CE-MS; refs. 12, 13). The major advantages of CE-MS analysis include its extremely high resolution, versatility to analyze metabolic profiles of various organisms, and ability to simultaneously quantify virtually all the charged low–molecular weight compounds in a sample (12, 14), which makes CE-MS best suited for the comprehensive analysis of energy metabolism in cells, tissues and biological fluids.

In the present study, we applied capillary electrophoresis time-of-flight mass spectrometry (CE-TOFMS; ref. 15) to the metabolome profiling of human colon and stomach cancers, and compared the metabolite levels in tumor and normal tissues obtained by surgery. The results clearly showed that the tumor microenvironment is far from ideal for cell growth from the viewpoint of energy metabolism, and showed the versatility of CE-MS–based metabolomics for global-scale analysis of energy metabolism in tissues.

Materials and Methods

Sample Collection and Metabolite Extraction

We conducted all the experiments according to the study protocol approved by the Institution Review Board of the National Cancer Center upon obtaining informed consent from all the subjects. Tumor and surrounding grossly normal-appearing tissues (Fig. 1) were obtained from 16 colon and 12 stomach cancer patients after surgical treatment. Patient and tumor stage information are listed in Table 1. The excised tissues were cut into <1-cm^3 pieces, immediately frozen in liquid nitrogen, and stored at −80°C until metabolite extraction.

To extract metabolites, preweighed deep-frozen samples (~50 mg each) were completely homogenized by a cell disrupter (MS-100R; TOMY) at 2°C, after adding 625 μL of methanol that contained internal standards [20 μmol/L each of methionine sulfone and 2-(N-morpholino)-ethanesulfonic acid]. The homogenate was then mixed with Milli-Q water and chloroform in a volume ratio of 5:2:5 and centrifuged at 9,000 *g* for 15 min at 4°C. Subsequently, the aqueous solution was centrifugally filtered through a 5-kDa cutoff filter (Millipore) to remove proteins. The filtrate was centrifugally concentrated and dissolved in 50 μL Milli-Q water that contained reference compounds (200 μmol/L each of 3-aminopyrrolidine and trimesate) immediately before CE-TOFMS analysis.

Reagents

Ophthalmate was purchased from BACHEM AG; glycerol-3-phosphate from Nakalai Tesque; sedoheptulose 7-phosphate from Glycoteam; tyramine, CoA, and NADH from MP Biomedicals; and fructose 1,6-bisphosphate, glucose 1-phosphate, ribose 5-phosphate, and ribulose 5-phosphate from Fluka. γ-Glu-Cys and γ-Glu-2-aminobutyrate were synthesized at the Toray Research Center. All other reagents were obtained from either Wako or Sigma-Aldrich. Stock solutions (1–100 mmol/L) were prepared in either Milli-Q water, 0.1 mol/L HCl, or 0.1 mol/L NaOH. All chemical standards were analytic or reagent grade. A mixed solution of the standards was prepared by diluting stock solutions with Milli-Q water immediately before CE-TOFMS analysis.

Analytic Condition for Metabolome Analysis

Instruments. All CE-TOFMS experiments were performed using an Agilent CE Capillary Electrophoresis System equipped with an Agilent TOFMS, an Agilent 1100 isocratic HPLC pump, an Agilent G1603A CE-MS adapter kit, and

Table 1. Patient information and tumor stages

	Characteristic	Colon		Stomach	
		Number	%	Number	%
Position of colon tumor	Rectum	10	63		
	Ascending colon	3	19		
	Transverse colon	1	6		
	Sigmoid colon	2	13		
Stage	I	5	31	2	17
	II	4	25	3	25
	III	6	38	5	42
	IV	1	6	2	17
Sex	Male	11	69	7	58
	Female	5	31	5	42

an Agilent G1607A CE–electrospray ionization (ESI)–MS sprayer kit (Agilent Technologies). For system control and data acquisition, we used Agilent G2201AA ChemStation software for CE and Analyst QS for TOFMS.

For measuring nucleotide derivatives, we used a CE-ESI-quadrupole MS system composed of an Agilent 1100 series MSD mass spectrometer equipped with the aforementioned other instruments. For the control and data acquisition in this system, we used Agilent 3D CE-MSD ChemStation software.

CE-TOFMS Conditions for Cationic Metabolite Analysis

Cationic metabolites were separated in a fused-silica capillary (50 μm i.d. × 100 cm total length) filled with 1 mol/L formic acid as the reference electrolyte (16). Sample solution was injected at 50 mbar for 3 s (~3 nL), and positive voltage of 30 kV was applied. The capillary and sample trays were maintained at 20°C and below 5°C, respectively. Sheath liquid that comprised methanol/water (50% v/v) that contained 0.5 μmol/L reserpine was delivered at 10 μL/min. ESI-TOFMS was operated in the positive ion mode. The capillary voltage was set at 4 kV and a flow rate of nitrogen gas (heater temperature 300°C) was set at 10 psig. In TOFMS, the fragmenter voltage, skimmer voltage, and octapole radio frequency voltage (Oct RFV) were set at 75, 50, and 125 V, respectively. An automatic recalibration function was performed by using two reference masses of reference standards; protonated methanol dimer ($[2\ \text{methanol} + H]^+$, *m/z* 65.059706) and protonated reserpine ($[M+H]^+$, *m/z* 607.280659), which provided the lock mass for exact mass measurements. Exact mass data were acquired at the rate of 1.5 cycles/s over a 50 to 1,000 *m/z* range.

CE-TOFMS Conditions for Anionic Metabolite Analysis

Anionic metabolites were separated in a cationic-polymer–coated SMILE(+) capillary (Nacalai Tesque) filled with 50 mmol/L ammonium acetate solution (pH 8.5) as the reference electrolyte (13). Sample solution was injected at 50 mbar for 30 s (~30 nL) and a negative voltage of −30 kV was applied. Ammonium acetate (5 mmol/L) in 50% methanol/water (50% v/v) that contained 1 μmol/L reserpine was delivered as sheath liquid at 10 μL/min. ESI-TOFMS was operated in the negative ion mode. The capillary voltage was set at 3.5 kV. In TOFMS, the fragmenter voltage, skimmer voltage, and Oct RFV were set at 100, 50, and 200 V, respectively. An automatic recalibration function was performed by using two reference masses of reference standards: deprotonated acetate dimer ($[2M-H]^-$, *m/z* 119.034984) and deprotonated reserpine ($[M-H]^-$, *m/z* 607.266107). Other conditions were identical to those used in cationic metabolome analysis.

CE-MS Conditions for Nucleotide-Related Metabolite Analysis

Separations were carried out in a fused-silica capillary (50 μm i.d. × 100 cm total length) filled with 50 mmol/L ammonium acetate solution (pH 7.5) as electrolyte (17). Before the first use, a new capillary was pretreated with preconditioning buffer, 25 mmol/L ammonium acetate/75 mmol/L sodium phosphate solution (pH 7.5), for 20 min. Before each injection, the capillary was equilibrated by flushing with the preconditioning buffer for 10 min and subsequently with the running buffer for 6 min, which was replenished every run using a buffer replenishment system equipped with the Agilent CE. Sample solution was injected at 50 mbar for 30 s (~30 nL). A voltage of +30 kV was applied and a pressure of 50 mbar was applied to the inlet capillary during the run (17). The capillary temperature was maintained at 20°C, and the sample tray was cooled to below 5°C. Ammonium acetate (5 mmol/L) in 50% methanol/water (v/v) was delivered as the sheath liquid at 10 μL/min. ESI-quadrupole MS was operated in the negative ion mode, and the capillary voltage was set at 3.5 kV. A flow of heated dry nitrogen gas (heater temperature 300°C) was switched off during the preconditioning step, and a pressure of 10 psig was applied 0.1 min after sample injection. Compounds were monitored using selective ion monitoring mode.

Liquid Chromatography Tandem Mass Spectrometry Conditions for Glucose Quantification

Liquid chromatography tandem mass spectrometry experiments were performed using an Agilent 1100 series HPLC system and an API3000 triple-quadrupole tandem mass spectrometer (Applied Biosystems), with the Applied Biosystems Analyst software for data acquisition. The separation was carried out on a TSKgel Amide-80 column (2.1 mm i.d. × 25 cm; Tosoh) and the mobile phase consisted of 75% acetonitrile and 25% Milli-Q water at a flow-rate of 0.2 mL/min. The temperature of the column oven was set at 80°C and 1-μL aliquots of the sample solution were injected into the column. Turbo spray mode was selected in the negative ion mode. Nebulizer gas pressure, air curtain gas pressure, nitrogen turbo gas temperature, and ion spray voltage were set at 12 psig, 6 psig, 500°C, and −4.5 kV, respectively. Multiple reaction monitoring detection was performed in MS/MS analysis to obtain sufficient selectivity and sensitivity.

CE-TOFMS Data Processing

Raw data were processed using in house software for the quantitation of metabolites. The overall data processing flow consists of the following steps; noise-filtering, baseline-correction, migration time alignment, peak detection, and integration of peak area from a 0.02 *m/z*-wide slice of the electropherograms, which resemble the strategies used in widely used data processing software for LC-MS and GC-MS data analysis such as MassHunter (Agilent Technologies) and XCMS (18). Subsequently, the accurate *m/z* of each peak was calculated by Gaussian curve fitting in the *m/z* domain, and migration times were normalized using alignment algorithms based on dynamic programming (15, 19). All target metabolites were identified by matching their *m/z* values and migration times with those of the standard compounds. Processed peak lists were exported for further statistical analysis.

Statistical Analysis

For each sample, the measured metabolite concentrations were normalized using tissue weight to obtain the amount of metabolite contained per gram of each sample. The Wilcoxon matched pairs test was used to compare metabolite levels in tumor and nontumor groups, to determine statistical significance. Z-score normalization was performed and heat maps of metabolite levels were generated using hierarchical clustering based on Pearson correlation coefficients using the MultiExperiment Viewer (MeV) software (Institute for Genomic Research; ref. 20).

Results and Discussion

Metabolome analyses of colon and stomach cancer tissues. We obtained pairs of surgically resected tumor and surrounding normal tissue samples from 16 colon and 12 stomach cancer patients and extracted metabolites for metabolome analysis. Surgically excised tissue samples were immediately frozen in liquid nitrogen, quickly weighed and immersed in methanol with internal standards, and completely homogenized at 2°C, which thus minimized sample degradation and halted potential enzymatic reactions during metabolite extraction process.

The CE-TOFMS systems in three different modes for cation, anion, and nucleotide analyses detected 738 (normal) and 877 (tumor) peaks in colon and 1007 (normal) and 1142 (tumor) peaks in stomach tissues on average, after eliminating redundant peaks, such as spike noises, fragments, and adduct ions. Among these, 94 peaks in colon and 95 peaks in stomach were identified and quantified with metabolite standards by matching the closest *m/z* values and normalized migration times for further statistical comparisons and interpretations. The identified metabolites and their quantities are listed in Supplementary Table S1 and graphically represented on a large-scale metabolome map (Supplementary Fig. S1).

The relative levels of metabolites in normal and tumor tissues obtained from colon and stomach cancer patients were visualized by using a hierarchical clustering algorithm (Supplementary Fig. S2). The normalized metabolome data were clustered according to metabolites vertically and samples horizontally. Two distinct metabolite clusters were observed in colon tissues: Most

metabolite levels including glycolytic intermediates, amino acids, some TCA and urea cycle intermediates, and nucleosides were higher in tumor tissues compared with their normal counterparts; however, these clusters were less distinguishable in stomach tissues. This trend was also present in the sample clusters: Colon samples were clearly separated into tumor and normal groups except for one normal sample clustered within the tumor group, whereas stomach samples were not well-separated. This indicates that tumor and normal stomach tissues were less distinguishable compared with colon tissues, according to the metabolome data obtained in this study. However, several key metabolites in energy metabolism, such as glucose and nucleoside triphosphates, were lower in both colon and stomach tumor tissues. No significant correlation was found between metabolite levels and the cancer stages of patients in both tissue types (data not shown).

Glycolysis and TCA cycle. As expected from the notion that cancer cells can deplete glucose in the hypovascular microenvironment caused by the hyperactivity of glycolysis, glucose concentrations were much lower in tumor than normal tissues in both types of cancers (Fig. 2). Mean glucose concentration of normal and tumor tissues was 1,220 ± 150 (mean ± SE) and 123 ± 43 nmol/g, respectively, in colon ($P = 0.0005$) and 1,290 ± 168 and 424 ± 131 nmol/g, respectively, in stomach ($P = 0.0068$) tissues. Concentrations of metabolites that are involved in glycolysis, pentose phosphate pathway, and TCA cycle are illustrated on a metabolic pathway map in Fig. 3. In colon and stomach cancer, tumor tissues contained nearly equal or higher amounts of glycolytic intermediates than their corresponding normal counterparts, and this trend was clearer in colon tissues. Scarce glucose and modest glucose 6-phosphate concentrations might result from the overexpression of glucose transporters (21) and particularly type II hexokinase expression (22), which are frequently observed in colon and stomach cancer. The accumulation of glucose 1-phosphate in colon cancer is also intriguing in that glycogen synthase kinase 3β expression is reportedly higher in colon cancer cell lines and colorectal cancer patients compared with their respective normal counterparts (23), which may result in the enhancement of glycogenolysis and a continuous supply of glucose 6-phosphate.

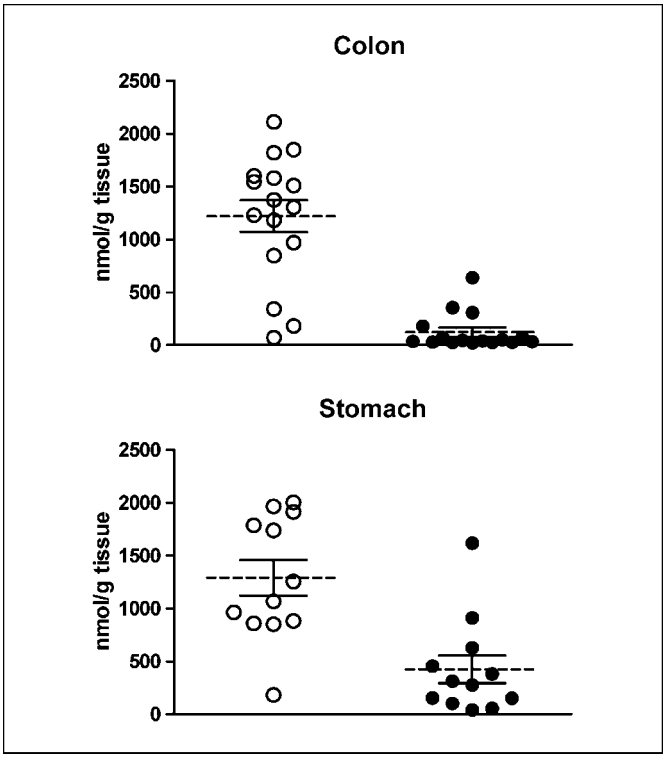

Figure 2. Quantified glucose concentrations of colon and stomach tissue samples. These data are individual glucose concentrations of normal and tumor samples each of colon and stomach subjects, with the mean concentrations (*dotted line*) ± SE.

In addition, pyruvate concentration is significantly lower in colon tumor and slightly lower in stomach tumor tissues, whereas lactate concentration in tumor tissues is higher in both tumor types than in their corresponding normal counterparts. This clearly indicates a high dependence of cancer cells on anaerobic breakdown of pyruvate. In particular, high lactate dehydrogenase 5 activity and resulting effective conversion of pyruvate to lactate have been identified in colon cancer (24, 25). Active glycolysis also increases the cytosolic $NADH/NAD^+$ ratio and thereby accelerates the activity of lactate dehydrogenase (26). Enhanced pyruvate-to-lactate conversion may also be due to the activation of pyruvate dehydrogenase kinase, isozyme 1 (PDK1) in cancer cells, which inactivates pyruvate dehydrogenase and leads to inactivation of the TCA cycle in cancer cells (27). Moreover, lactate accumulation creates a potentially favorable microenvironment for cancer cells to proliferate, as it causes local acidosis and potentially modulates the activity of proteases that decompose extracellular matrix, thereby liberating peptides and amino acids that are consumable for energy generation (28). Therefore, it is likely that cancer cells preferentially use glucose because of their intrinsic metabolic characteristics and microenvironmental aspects such as hypoxia. Moreover, extremely low glucose content in tumor tissues might result from poor blood supply and high glucose consumption by cancer cells.

If the density of soft tissues is assumed as 1 g/mL, our data indicate that the glucose concentration in tumor tissues is only ~1 of 45 (colon) or 1 of 13 (stomach) of the typical blood glucose concentration (1 mg/mL or 5.6 mmol/L). When cultured cancer cells are deprived of glucose, most conventional cytotoxic anticancer agents significantly lose their effectiveness (29). This is important when the pharmacologic effects of anticancer agents in the actual tumor microenvironment are considered since it was found to be significantly different from the typical glucose-rich medium that is commonly used for *in vitro* experiments. Accordingly, the present data imply that responses of most colon and stomach cancer cells against conventional anticancer drugs under the actual nutritionally poor *in vivo* environment could be considerably different from that which we expect from the data obtained under typical culture conditions.

Unexpectedly, significant organ-specific differences were also observed in the metabolite levels of the initial part of the TCA cycle, including acetyl CoA, citrate, *cis*-aconitate, iso-citrate, and 2-oxoglutarate, which were markedly lower in colon tissues. Interestingly, however, levels of the three TCA metabolites succinate, fumarate, and malate were comparable in colon and stomach tissues, whereas they were significantly higher in tumor samples in both cancers (Fig. 3). Wiesner and colleagues (30) have shown a decrease of citrate and 2-oxoglutarate and an increase of malate and succinate in anoxic rat heart myocytes. The trend of these TCA intermediate levels is consistent with our data obtained from colon tissues, presumably representing a typical metabolic fingerprint of hypoxic cells. In contrast, abundant TCA

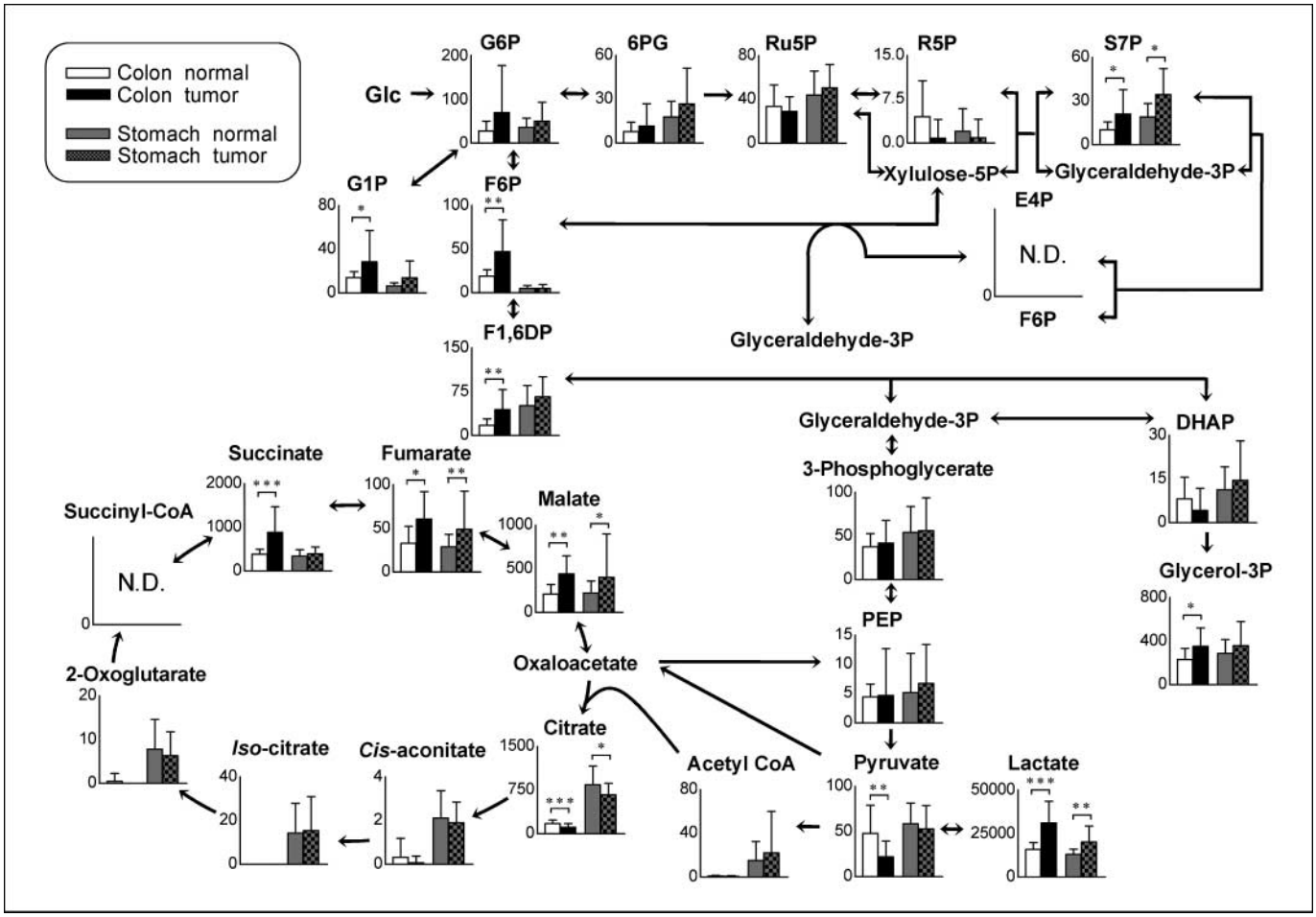

Figure 3. Quantified levels of metabolites involved in central carbon metabolism. Metabolite concentrations of colon and stomach tissues superimposed on a metabolic pathway map that included glycolysis, and the pentose phosphate and TCA pathways. *Columns,* average concentration (nmol/g tissue); *bars,* SD. *N.D.,* the metabolite concentration was below the detection limit of the analysis. All the *P* values were evaluated by the Wilcoxon matched pair test. *, $P < 0.05$; **, $P < 0.01$; ***, $P < 0.001$.

intermediates in stomach tissues, regardless of whether from tumor or normal tissues, imply active aerobic respiration via oxidative phosphorylation. It is uncertain, however, what causes the accumulation of fumarate and succinate in colon cancer tissues, despite extremely low concentrations of other TCA intermediates such as citrate and 2-oxoglutarate. In fact, it is known that some parasites and bacteria synthesize ATP without oxygen by using a reverse reaction of succinate dehydrogenase and produce succinate as a byproduct, which is so-called fumarate respiration, in which fumarate rather than molecular oxygen is used as electron acceptor (31, 32). Although the capability of mammalian cells to use fumarate respiration as an ATP generator has not been confirmed yet, we obtained strong evidence that the energy generation of cancer cells greatly depends on fumarate respiration under conditions of glucose deprivation and severe hypoxia.[3] Our data uncovered the metabolically unfavorable microenvironment of tumor tissues characterized by extremely low glucose availability under relatively hypoxic conditions in which the cells apparently rely on minimal aerobic respiration via the TCA cycle. Hence, the active use of fumarate respiration by cancer cells provides a likely and intriguing explanation for the accumulation of fumarate and succinate observed in colon tumor tissues.

Amino acids and nucleotides. Availability of amino acids is pivotal for cell proliferation because cancer cells are known to use some amino acids as energy sources (26). Free amino acids are mostly supplied to tissues via the bloodstream; thus, if blood supply to cancer tissues is considerably limited, amino acid content in tumor tissues may be lower compared with that in their normal counterparts. However, contrary to our expectations, levels of most amino acids and their primary derivatives were significantly higher in tumors than in normal colon and stomach tissues (Fig. 4). Among all the amino acids, however, an exception was glutamine; the colon and stomach tumor content of which was nearly equal to that in normal tissues. It has been pointed out that glutamine is a preferred amino acid for energy generation by cancer cells (33). High glutaminase activity and low glutamine synthase activity have been observed in several types of cancer cells (34). Because glutamate is the most abundant amino acid in tumor tissues, the conversion of glutamine to glutamate might be enhanced in tumor tissues.

One obvious question raised is the origin of these amino acids. Under limited blood supply, two main sources of amino acids can

[3] K. Kami et al. submitted for publication.

be conceived: one is the degradation of extracellular matrix particularly by matrix metalloproteinases and the other is the autophagic degradation of preexisting intracellular proteins. In this perspective, it is notable that hydroxyproline concentration was significantly higher in tumor tissues than in their normal counterparts (P = 0.0005 in colon and P = 0.0025 in stomach tissues). Hydroxyproline is abundant in collagen and is posttranslationally produced from proline, which suggests that the higher concentration of hydroxyproline in tumor tissues is indicative of excess degradation of collagen (35). Autophagy is another possible source of amino acids, as it is well-documented that autophagy liberates and thereby increases the free amino acid pools (36, 37). We also have found recently that autophagy seems essential for colon cancer cell survival (38) and is highly active in colon and pancreatic cancers (38, 39). Up-regulation of amino acid biosynthesis per se does not explain the accumulation of all the essential amino acids observed in tumor tissues. One might argue that all the amino acid levels seem to be higher in tumors because the number of cells contained in tumor tissues might have been greater than that in normal tissues, as cancer cells may have been highly aggregated. To rule out this possibility, we extracted DNA simultaneously with metabolites from each tissue and normalized our metabolome data with respect to the DNA content of each sample, and confirmed that the trend in amino acid levels did not change (data not shown).

The levels of most nucleotides such as ATP, ADP, GTP, and GDP in tumor and normal colon tissues were significantly lower than those in stomach tissues (Fig. 4). Nevertheless, no significant difference between colon and stomach tissues was observed with regard to the average adenylate energy charge (40), which is evaluated by the equation, [(ATP)+1/2(ADP)]/[(ATP)+(ADP)+(AMP)]. The low levels of most purine and pyrimidine compounds in colon tissues may indicate a relatively slower colon cell growth compared with stomach cells, as a recent study has shown that the nucleotide pools continuously decrease as the growth stage moves from the exponential to stationary phase in *Escherichia coli* (41). A challenging but intriguing alternative is that the levels of nucleotide pools may reflect the oxygen availability and its dependency in each tissue because hypoxic stress has been found to reduce purine and pyrimidine pools (42). The high-energy charge in colon tissues, despite the low total adenylate level, might be maintained by AMP deaminase reaction, which is known to stabilize the energy charge by decomposing adenylate (43). It is, however, remarkable that no significant difference between tumor and normal tissues was found for most nucleotide phosphates, total adenylate, and energy charge in either colon or stomach tissues. This implies that cancer cells have a growth advantage over their normal counterparts, not by securing more ATP and other building blocks for DNA synthesis, but rather by efficiently exploiting some strategic energy

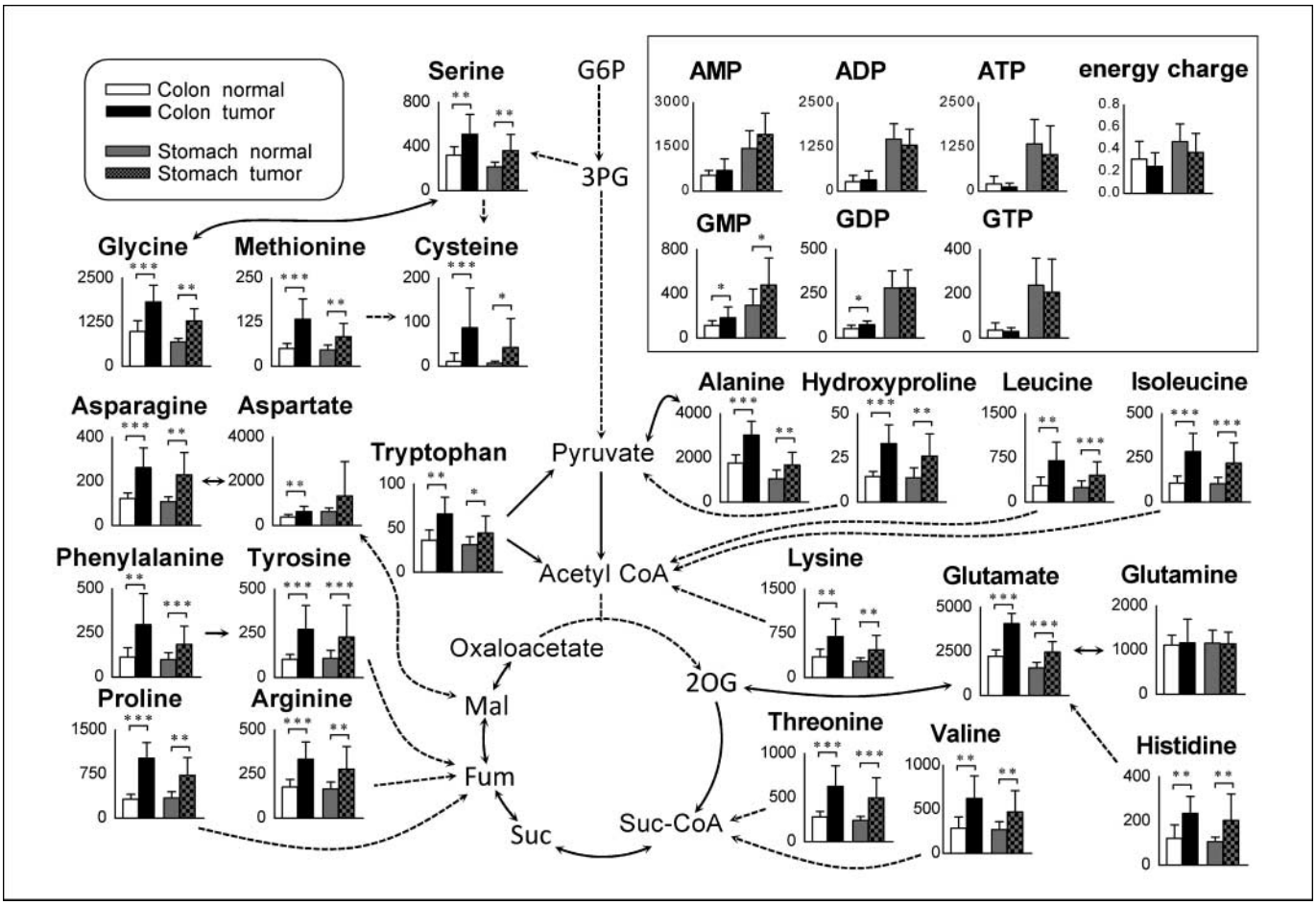

Figure 4. Metabolome data map of metabolites including amino acids, hydroxyproline, and nucleotides (shown in the box) in normal and tumor tissues obtained from colon and stomach cancer patients. *Columns,* average concentration (nmol/g tissue) of normal and tumor tissues; *bars,* SD. *N.D.,* the metabolite concentration was below the detection limit of the analysis. All the P values were evaluated by the Wilcoxon matched pair test. *, $P < 0.05$; **, $P < 0.01$; ***, $P < 0.001$.

metabolisms such as anaerobic glycolysis, glutaminolysis, autophagic production of amino acids, and possibly fumarate respiration, to maintain comparable levels of principal molecules in spite of limited resources and support continuous proliferation.

Intrasample variability and analytic limitations. Biochemical analysis of tissue samples is relatively difficult due to their high heterogeneity compared with cultured cells or body fluids. To examine the intrasample variability, we extracted metabolites from five different parts of a piece of colon or stomach tumor tissue and measured the metabolite levels by CE-TOFMS (Supplementary Table S2). The relative SDs of most metabolite levels were in the range of 6.7% to 40%. Given that the analytic variability of CE-MS is <5% (16), this relatively high intrasample variability may be attributed to a significantly high intratumor heterogeneity. Therefore, to minimize intrasample variability and thus maximize sensitivity for detecting tumor-specific or even tumor-stage specific metabolic differences, the use of laser capture microdissection for concentrating only the target cells before sample homogenization may be promising.

CE-MS is able to simultaneously quantify charged, low–molecular weight compounds and, thus, is suitable for the analysis of primary energy metabolism; however, it is not very effective for the separation of neutral compounds and macromolecules such as sugars, fats, cholesterols, steroid hormones, and long-chain peptides. Concomitant analysis of the same samples by LC-MS, GC-MS, and NMR approaches has the potential to greatly expand the coverage of target compounds and thereby increase the chance of finding molecular fingerprints of tumors and key markers of the tumorigenic process.

In the present study, we analyzed the metabolic state of tumor tissues in comparison with their normal counterparts and found that the nutritional conditions in the tumor microenvironment were far from ideal from the standpoint of energy metabolism. In particular, tumor glucose concentration was significantly lower than previously indicated (44). The results also indicate that tumors develop tumor-specific metabolism that endows them with more predominant proliferation, independent of tissue types, while retaining some metabolic traits of the tissues from which they originated. In other words, cancer cells are evolved through metabolic adaptation that involves primarily hyperactivation of glucose consumption and accumulation of amino acids, while retaining tissue-specific dependency of aerobic respiration represented by TCA intermediate and nucleotide levels. In conclusion, we analyzed the metabolome-wide tumor microenvironment and revealed cancer- and organ-specific characteristic energy metabolism by CE-TOFMS, which will be a vital technology for the future discovery of tissue-specific cancer biomarkers and for the awaited development of novel cancer therapeutic agents that target cancer-specific metabolic traits.

Disclosure of Potential Conflicts of Interest

No potential conflicts of interest were disclosed.

Acknowledgments

Received 12/17/08; revised 3/9/09; accepted 3/20/09; published OnlineFirst 5/19/09.

Grant support: Third Term Comprehensive 10-year Strategy for Cancer Control from the Ministry of Health, Labour and Welfare and a grant from the Global COE Program entitled, "Human Metabolomic Systems Biology." This work was also supported by KAKENHI (Grant-in-Aid for Scientific Research) on Priority Areas "Systems Genomes" and on "Lifesurveyor" from the Ministry of Education, Culture, Sports, Science and Technology of Japan as well as research funds from the Yamagata prefectural government and the City of Tsuruoka.

The costs of publication of this article were defrayed in part by the payment of page charges. This article must therefore be hereby marked *advertisement* in accordance with 18 U.S.C. Section 1734 solely to indicate this fact.

References

1. Vaupel P, Thews O, Kelleher DK, Konerding MA. O2 extraction is a key parameter determining the oxygenation status of malignant tumors and normal tissues. Int J Oncol 2003;22:795–8.
2. Warburg O. On the Origin of Cancer Cells. Science 1956;123:309–14.
3. Chen Z, Lu W, Garcia-Prieto C, Huang P. The Warburg effect and its cancer therapeutic implications. J Bioenerg Biomembr 2007;39:267–74.
4. Kondoh H. Cellular life span and the Warburg effect. Exp Cell Res 2008;314:1923–8.
5. Schauer N, Semel Y, Roessner U, et al. Comprehensive metabolic profiling and phenotyping of interspecific introgression lines for tomato improvement. Nat Biotechnol 2006;24:447–54.
6. Plumb R, Granger J, Stumpf C, Wilson ID, Evans JA, Lenz EM. Metabonomic analysis of mouse urine by liquid-chromatography-time of flight mass spectrometry (LC-TOFMS): detection of strain, diurnal and gender differences. Analyst 2003;128:819–23.
7. Opstad KS, Bell BA, Griffiths JR, Howe FA. An assessment of the effects of sample ischaemia and spinning time on the metabolic profile of brain tumour biopsy specimens as determined by high-resolution magic angle spinning 1H NMR. NMR Biomed 2008;21:1138–47.
8. Yang C, Richardson AD, Smith JW, Osterman A. Comparative metabolomics of breast cancer. Pac Symp Biocomput 2007:181–92.
9. Chan EC, Koh PK, Mal M, et al. Metabolic profiling of human colorectal cancer using high-resolution magic angle spinning nuclear magnetic resonance (HR-MAS NMR) spectroscopy and gas chromatography mass spectrometry (GC/MS). J Proteome Res 2009;8:352–61.
10. Denkert C, Budczies J, Kind T, et al. Mass spectrometry-based metabolic profiling reveals different metabolite patterns in invasive ovarian carcinomas and ovarian borderline tumors. Cancer Res 2006;66:10795–804.
11. Denkert C, Budczies J, Weichert W, et al. Metabolite profiling of human colon carcinoma-deregulation of TCA cycle and amino acid turnover. Mol Cancer 2008;7:72.
12. Soga T, Ohashi Y, Ueno Y, Naraoka H, Tomita M, Nishioka T. Quantitative metabolome analysis using capillary electrophoresis mass spectrometry. J Proteome Res 2003;2:488–94.
13. Soga T, Ueno Y, Naraoka H, Ohashi Y, Tomita M, Nishioka T. Simultaneous determination of anionic intermediates for Bacillus subtilis metabolic pathways by capillary electrophoresis electrospray ionization mass spectrometry. Anal Chem 2002;74:2233–9.
14. Sato S, Soga T, Nishioka T, Tomita M. Simultaneous determination of the main metabolites in rice leaves using capillary electrophoresis mass spectrometry and capillary electrophoresis diode array detection. Plant J 2004;40:151–63.
15. Soga T, Baran R, Suematsu M, et al. Differential metabolomics reveals ophthalmic acid as an oxidative stress biomarker indicating hepatic glutathione consumption. J Biol Chem 2006;281:16768–76.
16. Soga T, Heiger DN. Amino acid analysis by capillary electrophoresis electrospray ionization mass spectrometry. Anal Chem 2000;72:1236–41.
17. Soga T, Ishikawa T, Igarashi S, Sugawara K, Kakazu Y, Tomita M. Analysis of nucleotides by pressure-assisted capillary electrophoresis-mass spectrometry using silanol mask technique. J Chromatogr A 2007;1159:125–33.
18. Smith CA, Want EJ, O'Maille G, Abagyan R, Siuzdak G. XCMS: processing mass spectrometry data for metabolite profiling using nonlinear peak alignment, matching, and identification. Anal Chem 2006;78:779–87.
19. Baran R, Kochi H, Saito N, et al. MathDAMP: a package for differential analysis of metabolite profiles. BMC Bioinformatics 2006;7:530.
20. Saeed AI, Sharov V, White J, et al. TM4: a free, open-source system for microarray data management and analysis. Biotechniques 2003;34:374–8.
21. Koukourakis MI, Pitiakoudis M, Giatromanolaki A, et al. Oxygen and glucose consumption in gastrointestinal adenocarcinomas: correlation with markers of hypoxia, acidity and anaerobic glycolysis. Cancer Sci 2006;97:1056–60.
22. Pedersen PL, Mathupala S, Rempel A, Geschwind JF, Ko YH. Mitochondrial bound type II hexokinase: a key player in the growth and survival of many cancers and an ideal prospect for therapeutic intervention. Biochim Biophys Acta 2002;1555:14–20.
23. Shakoori A, Ougolkov A, Yu ZW, et al. Deregulated GSK3b activity in colorectal cancer: its association with tumor cell survival and proliferation. Biochem Biophys Res Commun 2005;334:1365–73.
24. Koukourakis MI, Giatromanolaki A, Polychronidis A, et al. Endogenous markers of hypoxia/anaerobic metabolism and anemia in primary colorectal cancer. Cancer Sci 2006;97:582–8.
25. Mazzanti R, Solazzo M, Fantappie O, et al. Differential expression proteomics of human colon cancer. Am J Physiol Gastrointest Liver Physiol 2006;290:G1329–38.

26. Argilés JM, Azcón-Bieto J. The metabolic environment of cancer. Mol Cell Biochem 1988;81:3–17.

27. Pan JG, Mak TW. Metabolic targeting as an anticancer strategy: dawn of a new era? Sci STKE 2007;381:pe14.

28. Brahimi-Horn MC, Chiche J, Pouysségur J. Hypoxia signalling controls metabolic demand. Curr Opin Cell Biol 2007;19:223–9.

29. Lu J, Kunimoto S, Yamazaki Y, Kaminishi M, Esumi H. Kigamicin D, a novel anticancer agent based on a new anti-austerity strategy targeting cancer cells' tolerance to nutrient starvation. Cancer Sci 2004;95:547–52.

30. Wiesner RJ, Kreutzer U, Rosen P, Grieshaber MK. Subcellular distribution of malate-aspartate cycle intermediates during normoxia and anoxia in the heart. Biochim Biophys Acta 1988;936:114–23.

31. Kita K, Hirawake H, Miyadera H, Amino H, Takeo S. Role of complex II in anaerobic respiration of the parasite mitochondria from Ascaris suum and Plasmodium falciparum. Biochim Biophys Acta 2002;1553:123–39.

32. Ullmann R, Gross R, Simon J, Unden G, Kroger A. Transport of C4-dicarboxylates in Wolinella succinogenes. J Bacteriol 2000;182:5757–64.

33. Medina MA, Sánchez-Jiménez F, Márquez J, Rodríguez Quesada A, Núñez de Castro I. Relevance of glutamine metabolism to tumor cell growth. Mol Cell Biochem 1992;113:1–15.

34. Moreadith RW, Lehninger AL. The pathways of glutamate and glutamine oxidation by tumor cell mitochondria. Role of mitochondrial NAD(P)+-dependent malic enzyme. J Biol Chem 1984;259:6215–21.

35. Phang JM, Donald SP, Pandhare J, Liu Y. The metabolism of proline, a stress substrate, modulates carcinogenic pathways. Amino Acids 2008;35:681–90.

36. Droge W. Autophagy and aging-importance of amino acid levels. Mech Ageing Dev 2004;125:161–8.

37. Mizushima N, Klionsky DJ. Protein turnover via autophagy: implications for metabolism. Annu Rev Nutr 2007;27:19–40.

38. Sato K, Tsuchihara K, Fujii S, et al. Autophagy is activated in colorectal cancer cells and contributes to the tolerance to nutrient deprivation. Cancer Res 2007;67:9677–84.

39. Fujii S, Mitsunaga S, Yamazaki M, et al. Autophagy is activated in pancreatic cancer cells and correlates with poor patient outcome. Cancer Sci 2008;99:1813–9.

40. Chapman AG, Fall L, Atkinson DE. Adenylate energy charge in Escherichia coli during growth and starvation. J Bacteriol 1971;108:1072–86.

41. Buckstein MH, He J, Rubin H. Characterization of nucleotide pools as a function of physiological state in *Escherichia coli*. J Bacteriol 2008;190:718–26.

42. Hisanaga K, Onodera H, Kogure K. Changes in levels of purine and pyrimidine nucleotides during acute hypoxia and recovery in neonatal rat brain. J Neurochem 1986;47:1344–50.

43. Chapman AG, Atkinson DE. Stabilization of adenylate energy charge by the adenylate deaminase reaction. J Biol Chem 1973;248:8309–12.

44. Gatenby RA, Smallbone K, Maini PK, et al. Cellular adaptations to hypoxia and acidosis during somatic evolution of breast cancer. Br J Cancer 2007;97:646–53.